Magnetostriction, magnetoelastic coupling, and the magnetic Grüneisen constant in the antiferromagnet $RbMnF_3$

Y. Shapira and N. F. Oliveira, Jr.*
Francis Bitter National Magnet Laboratory, Massachusetts Institute of Technology, Cambridge, Massachusetts 02139
(Received 9 March 1978)

The magnetostriction in $RbMnF_3$ (a cubic low-anisotropy Heisenberg antiferromagnet) was measured at 4.2 K in magnetic fields H up to 137 kOe. Capacitance dilatometers were used. The change Δl in the length l along the [001] direction was measured with $\vec{H}$ parallel to the [001], [100], or [110] directions. Two distinct phenomena were observed. At low fields, of order 1 kOe, l underwent a fractional change of order 1×10^{-6}. The sign and magnitude of this change depended on the direction of $\vec{H}$. This low-field magnetostriction is related to the H-induced reorientation of the sublattice magnetizations (analogous to the spin-flop transition), and is interpreted quantitatively in terms of a model for the magnetoelastic coupling in $RbMnF_3$ which was originally proposed by Eastman *et al.* The low-field magnetostriction data for $\vec{H}\parallel[001]$ and $\vec{H}\parallel[100]$ lead to the values $b_1=(1.88\pm0.15)\times10^6$ and $(1.77\pm0.14)\times10^6$ erg/cm^3, respectively, for the dominant magnetoelastic coupling constant. These values are in agreement with other determinations of b_1. In fields above several kilo-oersted, l increased linearly with H^2, with a slope $d(\Delta l/l)/d(H^2)=4\times10^{-16}$ Oe^{-2} which was the same (within the experimental error) for $\vec{H}\parallel[001]$ and $\vec{H}\parallel[100]$. This high-field magnetostriction is related to the H-induced canting of the sublattice magnetizations and the concomitant change in the exchange energy. The high-field magnetostriction arises from the dependence of the dominant exchange "constant" J on the volume V. Analysis of the data yields a magnetic Grüneisen constant $\gamma_{mag}=-(\partial\ln J/\partial\ln V)=4.5\pm0.4$. This value corresponds to $\partial T_N/\partial P=0.53\pm0.05$ K/kbar, where T_N is the Néel temperature and P is the hydrostatic pressure. At zero pressure, $T_N=83.03\pm0.03$ K for our sample. Our value for γ_{mag} agrees well with most other data which are related to this parameter, but is inconsistent with the thermal-expansion data of Teaney *et al.* Our own thermal-expansion data agree with the value of γ_{mag} obtained from the magnetostriction data. Detailed calculations of the low- and high-field magnetostriction are presented. The similarity between the underlying mechanisms responsible for the magnetostriction of antiferromagnets and ferromagnets is discussed.

I. INTRODUCTION

Magnetostriction is the lattice deformation which accompanies a change in the state of magnetization, and is usually studied experimentally by measuring the change in the dimensions of the sample as a function of magnetic field $\vec{H}$. The great majority of experimental studies of the magnetostriction have been carried out on ferromagnets; only a few experiments were performed on antiferromagnets. Here, we present a study of the magnetostriction in the simple antiferromagnet $RbMnF_3$. Although many features of the magnetostriction in $RbMnF_3$ are characteristic of the antiferromagnetic order, the basic interactions which give rise to this magnetostriction are similar to those responsible for the magnetostriction in the more familiar case of ferromagnets. The interpretation of the experimental results in $RbMnF_3$ will therefore be based on an extension of treatments of magnetostriction in ferromagnets.

When a magnetic field is applied to a ferromagnet at a temperature T below the Curie temperature T_C, the magnetization $\vec{M}$ in each domain tends to align parallel to $\vec{H}$. For sufficiently high H (often, no more than several kOe), the total magnetization of the sample reaches technical saturation and is parallel to $\vec{H}$. The magnetostriction which accompanies domain alignment, and the dependence of the magnetostriction above technical saturation on the direction of $\vec{H}$ relative to the crystal axes, have been the major topics of the standard discussions of magnetostriction in ferromagnets.[1,2] These discussions will be extended here to interpret the magnetostriction associated with spin reorientation in $RbMnF_3$.

Another cause for the magnetostriction in ferromagnets is the H-induced change in the magnitude of $\vec{M}$ (rather than the change in the direction of $\vec{M}$ relative to the crystal axes). The change in the magnitude of $\vec{M}$ is accompanied by a change in the exchange energy. The dependence of the exchange energy on elastic strain then leads to "exchange magnetostriction." This type of magnetostriction was recently studied in the cubic ferromagnet EuO above T_C.[3] A process which is analogous to the H-induced exchange magnetostriction is the lattice deformation which occurs when a ferromagnet is cooled (at $H=0$) from a temperature well above T_C to a temperature well below T_C. The development of a spontaneous magnetization in each domain is then accompanied by a change in the exchange energy, and by a corresponding lattice deformation. The common physical origin of the

magnetic thermal expansion and the H-induced exchange magnetostriction was emphasized in the theoretical treatment of Callen and Callen.[4,5] A convincing experimental confirmation of these theoretical ideas is the work of Argyle *et al.*[6] on the magnetic thermal expansion of EuO.

The exchange magnetostriction in ferromagnets has its counterpart in antiferromagnets such as $RbMnF_3$. However, the exchange magnetostriction in antiferromagnets has some distinctive features. For example, the exchange energy of an antiferromagnet at $T=0$ is H dependent. This gives rise to an H-induced exchange magnetostriction at $T=0$. In contrast, at $T=0$ the exchange energy of a simple ferromagnet with localized spins is saturated, and is, therefore, H independent. For such a ferromagnet there is no H-induced exchange magnetostriction at $T=0$.

Only a few experimental studies of the magnetostriction in antiferromagnets have been made.[5] The main reason for this is the relatively small response of many antiferromagnets to an external magnetic field. That is, very high magnetic fields are often required to change the orientations of the sublattice magnetizations of an antiferromagnet significantly, or to produce a net magnetization which is a significant fraction of the saturation magnetization. Callen[5] quotes several magnetostriction studies in which the magnetic field was insufficient to cause a complete reorientation of the sublattice magnetizations (i.e., realignment of the antiferromagnetic domains). Among these is the work of Albert and Lee[7] on NiO, in which fields up to 21 kOe were used. An example of a magnetostriction study in which the magnetic field was sufficiently high to cause a complete reorientation of the sublattice magnetizations (relative to the crystal axes) is the work of Levitin *et al.*[8] on α-Fe_2O_3. This study includes the magnetostriction associated with the spin-flop transition, where the sublattice magnetizations change their orientations abruptly from the easy axis to a direction perpendicular to it. The magnetostriction near the spin-flop transition was also studied in Cr_2O_3 (Refs. 9 and 10) and in $CsMnCl_3 \cdot 2H_2O$ (Ref. 11). The spin-flop transition is of first order. The behavior of the magnetostriction near second-order transitions was studied experimentally in a few cases.[10-12] The H-induced exchange magnetostriction was investigated in MnF_2 at temperatures near and above the Néel temperature T_N.[12-14] The magnetic thermal expansion at $H=0$ was studied in several antiferromagnets and was interpreted in terms of the strain dependence of the exchange energy.[15] In type-II fcc antiferromagnets, the anisotropic part of the thermal expansion leads to a change in the symmetry of the crystal, which occurs as the antiferromagnetic order is established.

$RbMnF_3$ is a cubic antiferromagnet with $T_N = 83$ K. This material has many attractive properties which make it a favorable choice for experimental tests of theories concerning antiferromagnets. The magnetic ion in $RbMnF_3$ is Mn^{++}, whose ground state has a zero orbital angular momentum and spin $S=\frac{5}{2}$. The Mn^{++} ions form a simple cubic lattice. In the antiferromagnetic phase each of these ions is surrounded by six nearest-neighbor magnetic ions which are on the opposite sublattice. Thus, a simple two-sublattice model is applicable. The dominant exchange interaction is between ions which are nearest neighbors; all other exchange interactions are considerably weaker.[16] The cubic anisotropy favors the $\langle 111 \rangle$ equivalent directions, but is extremely small. At 4.2 K, the anisotropy field H_A is approximately 4.5 Oe, compared to an exchange field $H_E \cong 8 \times 10^5$ Oe.[16-18] These properties make $RbMnF_3$ one of the best examples of the ideal isotropic Heisenberg antiferromagnet with nearest-neighbor interactions only.[19]

In this paper we report on a study of the magnetostriction in $RbMnF_3$ at 4.2 K and in fields up to 137 kOe. Two magnetostrictive phenomena are discussed. The first is the magnetostriction associated with the H-induced reorientation of the sublattice magnetizations relative to the crystal axes (without an appreciable change in their antiparallel orientation relative to each other). This reorientation process (or domain alignment) is completed in fields of several kOe. The second phenomenon is the magnetostriction at higher fields, which is predominantly an exchange magnetostriction. Both phenomena are interpreted in terms of models which are analogous to those used in ferromagnets. Analysis of the low-field magnetostriction yields the strength of the dominant magnetoelastic constant, whereas that of the high-field magnetostriction yields the magnetic Grüneisen constant (i.e., the volume dependence of the exchange "constant").

The paper is arranged as follows. After a description of the experimental techniques in Sec. II, the two major magnetostrictive phenomena are discussed qualitatively in Sec. III. Detailed quantitative discussions of the low- and high-field magnetostrictions are given in Secs. IV and V, respectively. Each of these two sections contains a theoretical subsection which is followed by experimental results and an analysis of these results in terms of the theory.

II. EXPERIMENTAL TECHNIQUES

Magnetostriction measurements were performed on a $RbMnF_3$ single crystal grown by the Crystal

Physics Group, Center for Materials and Engineering, MIT. The sample was a rectangular parallelepiped with faces parallel to the {100} planes. The linear dimensions of the sample were 5× 5× 7 mm. In the experiments, the linear dimension of the sample along the [001] direction (approximately 7 mm) was measured as a function of magnetic field $\vec{H}$. The Néel temperature of this sample was $T_N = 83.03 \pm 0.03$ K.

The magnetostriction was measured with two capacitance dilatometers, similar to those described in Ref. 3. The manner in which the sample was held in place is of some importance in the interpretation of the data. In our experimental setup, the sample was placed between a stationary brass frame and a spring-loaded movable brass plate. Thus, the sample was subjected to a small uniaxial pressure (approximately 14 bar). This pressure was sufficient for holding the sample firmly against the brass frame. A change in the length of the sample produced a movement of the spring-loaded plate. This movement was detected as a change in the capacitance between the moving plate and another stationary brass plate which was mechanically attached to the frame. The two plates of the capacitor were approximately 0.1 mm apart, and the capacitance was approximately 8 pF. It is important to note that no glue of any kind was used to hold the sample in place, so that there were no mechanical constraints on the dimensions of the sample.

The capacitance cell of each dilatometer was surrounded by a copper can filled with helium exchange gas. All the data were taken at 4.2 K with the copper can immersed in a liquid-helium bath. The performance of the capacitance dilatometers was checked by measuring the magnetostriction of a polycrystalline nickel sample and comparing the results with known values.[20] In addition, the background signal for each dilatometer was measured in fields up to 137 kOe by replacing the $RbMnF_3$ sample by "nonmagnetic" samples (copper and glass). For fields below ~ 4 kOe, the background was negligible compared with the signal from the $RbMnF_3$ sample. However, for the high-field data in $RbMnF_3$ it was necessary to apply a background correction. The high-field background had roughly the same H dependence as that of the signal from the $RbMnF_3$ sample. The magnitude of the background correction was ~ 4% for data obtained with one dilatometer, and ~ 7% for data obtained with the other.

The magnetostriction measurements for each of several experimental configurations were repeated several times. Below, each quoted magnitude of the magnetostriction for a given experimental configuration is an average over all runs for this configuration. Based on the reproducibility of the data, the reproducibility of the background, and the checks with the nickel sample, we estimate that the uncertainty in the quoted magnitudes of the various magnetostrictive effects was 8%.

Two magnets were used in the present work: a high-field Bitter magnet with a maximum field of 140 kOe, and a 9-in. Varian electromagnet with a maximum field of 12 kOe. The applied magnetic field was known with an accuracy of 0.3%. The magnitude of the demagnetizing field was between 0.1% and 0.2% of the applied magnetic field, depending on the orientation of $\vec{H}$ relative to the sample. We chose to ignore this small demagnetizing field, i.e., the internal magnetic field was assumed to be equal to the applied field.

A nonuniform magnetic field produces a force on the sample. Such a force may move the sample slightly, thereby changing the signal from a capacitance dilatometer used to measure the magnetostriction of the sample. As a check, the measurements in the Bitter magnet were repeated with the sample (and the dilatometer) displaced from the nominal magnetic center by up to 1.5 cm. Such a displacement should have increased the field gradient, and hence the magnetic force. No noticeable effect of the displacement on the magnetostriction data was observed. A similar check was not carried out in the case of the high-homogeneity Varian magnet. The data in the Varian magnet were taken only below 9 kOe, and were in very good agreement with those obtained in the Bitter magnet for the same range of magnetic fields.

We have also considered the possibility of a magnetic torque on the sample, which might have given rise to a spurious signal. The effect of such a torque was expected to be small, for two reasons: (i) All measurements were made with $\vec{H}$ along a symmetry axis, for which the torque should vanish. Thus, a torque could have occurred only due to a small unintentional field misalignment. (ii) For fields above the spin-flop field (of order 2.5 kOe, as discussed later) the magnetic susceptibility of $RbMnF_3$ should be very nearly independent of the direction of $\vec{H}$. Therefore, at these fields the torque is expected to be small for any direction of $\vec{H}$. Thus, even if $\vec{H}$ is not along a symmetry direction, all data above ~ 2.5 kOe (and also the measured change in length between $H = 0$ and any field above ~ 2.5 kOe) should not be significantly affected by the torque. Experimentally, we have checked the possible effect of a magnetic torque on our data by purposely tilting the magnetic field away from the symmetry direction by ~ 3°. No effect of this purposeful field misalignment on the magnetostriction data was observed.

III. QUALITATIVE FEATURES OF THE MAGNETOSTRICTION

At temperatures below T_N, the magnetostriction in $RbMnF_3$ exhibits two distinct effects which are caused by different physical mechanisms. The purpose of the present section is to introduce these two effects and to discuss the mechanisms responsible for them in qualitative terms. Detailed quantitative discussions are given in Secs. IV and V.

Let l be the length of the sample along the direction of the unit vector $\hat{l}$. The isothermal magnetostriction $(\Delta l/l)$ is the fractional change in l caused by the application of a magnetic field $\vec{H}$ at a constant temperature, i.e.,

$$\Delta l/l = [l(H) - l(0)]/l(0) . \quad (1)$$

In general, $\Delta l/l$ depends on the direction of $\hat{l}$, on the magnitude and direction of $\vec{H}$, and on the temperature T. In the present paper we report only on experiments at $T = 4.2$ K, so that the T dependence of the magnetostriction need not be considered. Also, in the present work $\hat{l}$ was always parallel to the [001] direction.

Figure 1 shows the magnetostriction as a function of H for the "longitudinal" configuration, with both $\hat{l}$ and $\vec{H}$ parallel to the [001] direction. These data exhibit two distinct effects: (i) a rapid change of $l(H)$ in fields of order 1 kOe, and (ii) a monotonic change of l with increasing H at higher fields. Other data show that the sign of the H-induced change of l in fields of ~ 1 kOe depends on the direction of $\vec{H}$. For fields well above 1 kOe, l always increases with increasing H. The two magnetostrictive effects are related to the H-induced changes in the orientations of the sublattice magnetizations $\vec{M}_1$ and $\vec{M}_2$. The first effect (at low fields) is related to the reorientation of $\vec{M}_1$ and $\vec{M}_2$ relative to the crystal axes, which occurs without an appreciable change in the angle between $\vec{M}_1$ and $\vec{M}_2$. The second effect (at high fields) is related to the change in the angle between $\vec{M}_1$ and $\vec{M}_2$.

At $H = 0$, $\vec{M}_1$ and $\vec{M}_2$ are equal in magnitude but opposite in direction, and are directed along one of the equivalent ⟨111⟩ directions. Because there are four equivalent ⟨111⟩ directions, there are four types of antiferromagnetic domains. We consider the effect of a magnetic field, applied along [001], on the orientations of $\vec{M}_1$ and $\vec{M}_2$. For this direction of $\vec{H}$ the behavior of all the domains is similar, so that it is sufficient to consider one domain with sublattice magnetizations initially along the [111] direction. Figure 2 schematically shows the dependence of the orientation of $\vec{M}_1$ and $\vec{M}_2$ on H. At low fields, $\vec{M}_2$ remains very nearly antiparallel to $\vec{M}_1$, but the orientations of $\vec{M}_1$ and $\vec{M}_2$ relative to the crystallographic axes change. This low-field reorientation of the sublattice magnetizations is analogous to the spin-flop transition in uniaxial antiferromagnets, and is completed at a field H_{sf} which is equal approximately to 2.5 kOe at 4.2 K. At H_{sf}, the sublattice magnetizations are parallel to the [110] axis, which is perpendicular to $\vec{H}$. The rapid change of l, in fields of ~ 1 kOe, is caused by the low-field reorientation of the antiparallel sublattice magnetizations. The physical interaction which links the length l to the orientations of $\vec{M}_1$ and $\vec{M}_2$ is the magnetoelastic coupling. An analogous situation exists in ferromagnets, where the

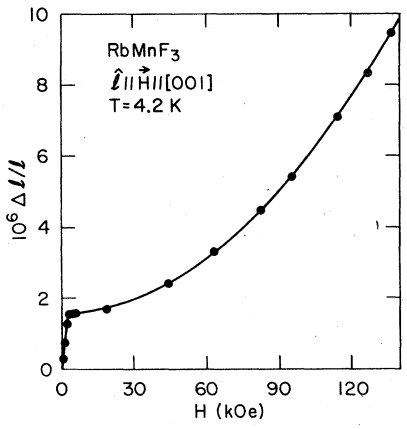

FIG. 1. Longitudinal magnetostriction of $RbMnF_3$ at 4.2 K. $\Delta l/l = [l(H) - l(0)]/l(0)$ is the fractional change in the length l caused by a magnetic field $\vec{H}$. These data are for the configuration $\hat{l} \parallel \vec{H} \parallel [001]$, where $\hat{l}$ is a unit vector which specifies the crystallographic direction along which the length is measured.

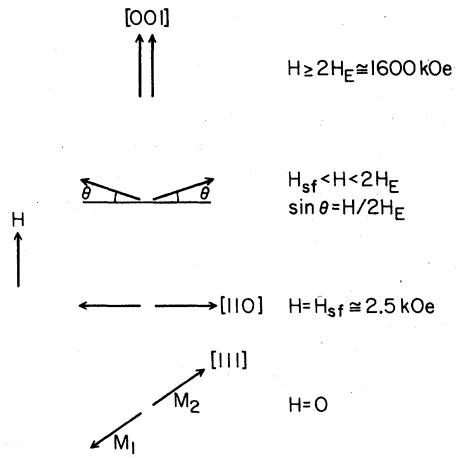

FIG. 2. Schematic illustration of the orientations of the sublattice magnetizations $\vec{M}_1$ and $\vec{M}_2$ at various values of H. This schematic is for a [111] domain, with $\vec{H}$ parallel to the [001] direction.

magnetoelastic coupling is responsible for the magnetostriction associated with alignment of ferromagnetic domains by an external magnetic field.[1,2]

In fields above H_{sf}, the sublattice magnetizations are canted relative to each other. The canting angle 2θ increases with increasing H. Ultimately, when H reaches $2H_E$ the sublattice magnetizations become parallel to each other and a phase transition from the antiferromagnetic to the paramagnetic phase takes place.[21] For $RbMnF_3$ at 4.2 K, $2H_E \cong 1600$ kOe, which is well above the fields used in the present experiments. The increase of the canting angle with increasing H is accompanied by an increase of l, i.e., the high-field magnetostriction in Fig. 1 is caused by the gradual change in the canting angle. The coupling mechanism responsible for this magnetostriction arises from the dependence of the exchange "constant" on elastic strain. The equilibrium elastic strain is determined by the minimum of the free energy, which contains contributions from the exchange energy and from the purely elastic energy. With increasing canting angle, the exchange energy (proportional to $\vec{M}_1 \cdot \vec{M}_2$) changes, which, in turn, leads to a change in the equilibrium strain.

IV. MAGNETOSTRICTION AT LOW FIELDS

In this section we consider the magnetostriction of $RbMnF_3$ at low H, i.e., between $H=0$ and $H \simeq 4$ kOe. This magnetostriction is related to the H-induced reorientation of the sublattice magnetizations, and is interpreted in terms of the magnetoelastic interaction in $RbMnF_3$ which was first considered by Eastman *et al.*[22,23]

A. Equilibrium orientations of the sublattice magnetizations

In the ordered phase and at $H=0$, $\vec{M}_1$ and $\vec{M}_2$ are antiparallel to each other and are directed along one of the $\langle 111 \rangle$ axes. As H is increased from zero, the sublattice magnetizations rotate towards the plane perpendicular to $\vec{H}$. The H dependence of the equilibrium orientations of $\vec{M}_1$ and $\vec{M}_2$ was treated by several authors.[24-26] The following discussion is based largely on these treatments. Although this discussion applies to all temperatures below T_N, the numerical values which are quoted below are for $T=4.2$ K, which is the temperature at which the present experiments were performed.

1. Anisotropy energy

Consider a $RbMnF_3$ sample at zero external mechanical stress and with a volume of 1 cm^3. The anisotropy energy E_A (defined as the anisotropic part of the Gibbs-like free energy at zero stress[2]) is assumed to have the form

$$E_A = K[(\alpha_1^2\alpha_2^2 + \alpha_2^2\alpha_3^2 + \alpha_3^2\alpha_1^2) + (\beta_1^2\beta_2^2 + \beta_2^2\beta_3^2 + \beta_3^2\beta_1^2)], \quad (2)$$

where α_i and β_i are the direction cosines of $\vec{M}_1$ and $\vec{M}_2$, respectively, relative to the cubic crystallographic axes. The fact that the $\langle 111 \rangle$ axes are the easy axes implies that $K<0$. The anisotropy field H_A is related to K as $H_A = -4K/3M_s$, where M_s is the magnitude of $\vec{M}_1$ or $\vec{M}_2$.

For fields below ~ 4 kOe, $\vec{M}_1$ is very nearly antiparallel to $\vec{M}_2$. (The angle 2θ between $\vec{M}_1$ and $-\vec{M}_2$ is less than 0.3° for $H<4$ kOe.) Thus, for these low fields, $\beta_i \cong -\alpha_i$. To a good approximation, the orientations of $\vec{M}_1$ and $\vec{M}_2$ are then specified by the orientation of the staggered magnetization $\vec{L} = \vec{M}_1 - \vec{M}_2$. If γ_i are the direction cosines of $\vec{L}$, then $\alpha_i \cong \gamma_i$ and $\beta_i \cong -\gamma_i$. The anisotropy can then be approximated as

$$E_A \cong 2K(\gamma_1^2\gamma_2^2 + \gamma_2^2\gamma_3^2 + \gamma_3^2\gamma_1^2). \quad (3)$$

Equation (3) is similar to the standard expression for the anisotropy in a cubic ferromagnet,[1] except that the staggered magnetization $\vec{L}$ plays the role of the magnetization $\vec{M}$ in a ferromagnet.

2. Antiferromagnetic domains

At $H=0$, $\vec{L}$ is parallel to one of the equivalent $\langle 111 \rangle$ directions. Because all the $\langle 111 \rangle$ directions are energetically equivalent, the staggered magnetizations in different regions of the sample may be parallel to different $\langle 111 \rangle$ directions, i.e., the sample may contain different domains. There are four types of such domains, with $\vec{L}$ parallel to [111], [11$\bar{1}$], [1$\bar{1}$1], and [$\bar{1}$11]. Here we chose to ignore the distinction between a domain with $\vec{L} \parallel [111]$ and a domain with $\vec{L} \parallel [\bar{1}\bar{1}\bar{1}]$, because the latter is obtained from the former by interchanging the labels 1 and 2 for the two sublattices.

For a nonzero H, the staggered magnetization (in a given domain) usually is not parallel to a $\langle 111 \rangle$ direction. Nevertheless, in order to distinguish between the four types of domains, they will be labelled in terms of the orientation of $\vec{L}$ at $H=0$. Thus, a domain with $\vec{L} \parallel [111]$ at $H=0$ will be referred to as a [111] domain, etc.

For a given domain in a field $\vec{H}$, the equilibrium orientation of $\vec{L}$ is determined by the competition between two mechanisms: the anisotropy which tends to orient $\vec{L}$ parallel to a $\langle 111 \rangle$ axis, and the field $\vec{H}$ which favors configurations with $\vec{L}$ perpendicular to $\vec{H}$. To interpret the present experiments it is sufficient to consider the theoretical results[24-26] for only two orientations of $\vec{H}$, namely, $\vec{H} \parallel [001]$ and $\vec{H} \parallel [110]$.

3. $\vec{H} \parallel [001]$

In this case, $\vec{H}$ makes equal angles with all the $\langle 111 \rangle$ equivalent directions. Therefore, the behavior of all four types of domains is similar. We focus first on the [111] domain. As H is increased from zero, $\vec{L}$ rotates towards the [110] direction, which is a direction with minimum anisotropy energy in the plane perpendicular to $\vec{H}$. Detailed calculations[24-26] show that $\vec{L}$ becomes parallel to [110] when H reaches the characteristic field $H_{sf} = (1.5 H_A H_E)^{1/2} = 2.3$ kOe. (Our experimental value is $H_{sf} \cong 2.5$ kOe.) This characteristic field is analogous to the spin-flop field in a uniaxial antiferromagnet,[27] but in contrast to the uniaxial case there is no abrupt change in the orientation of $\vec{L}$ at H_{sf}, i.e., $RbMnF_3$ does not exhibit a first-order transition at H_{sf}. For H above H_{sf}, $\vec{L}$ remains parallel to the [110] direction.

For a $[11\bar{1}]$ domain, the orientation of $\vec{L}$ in fields above H_{sf} is the same as for a [111] domain, namely, $\vec{L} \parallel [1\bar{1}0]$. For the $[\bar{1}11]$ and $[1\bar{1}1]$ domains, the staggered magnetization in fields above H_{sf} is parallel to the $[1\bar{1}0]$ direction.

4. $\vec{H} \parallel [110]$

In this case $\vec{H}$ is perpendicular to the $[\bar{1}11]$ and $[1\bar{1}1]$ directions, but not to the [111] and $[11\bar{1}]$ directions. As a result, the behavior of the $[\bar{1}11]$ and $[1\bar{1}1]$ domains is different from that of the [111] and $[11\bar{1}]$ domains.

Consider first the $[\bar{1}11]$ and $[1\bar{1}1]$ domains. Because the $[\bar{1}11]$ and $[1\bar{1}1]$ directions are perpendicular to $\vec{H}$ and, at the same time, are directions of minimum anisotropy energy, the orientation of $\vec{L}$ will not be affected by H. These domains are, therefore, stable and will persist to high fields.

In contrast, the [111] and $[11\bar{1}]$ domains become unstable when a sufficiently high field is applied, i.e., the direction of $\vec{L}$ in these regions of the sample will switch to one of the two $\langle 111 \rangle$ directions which are perpendicular to $\vec{H}$. Theoretical calculations[24] show that the [111] and $[11\bar{1}]$ domains cannot exist above 2.0 kOe. Some experimental data[24] suggest that these domains disappear in fields as low as several hundred Oe.

In summary, for fields above 2.0 kOe (and possibly even at lower fields) the staggered magnetization in all regions of the sample is parallel to either the $[\bar{1}11]$ or $[1\bar{1}1]$ directions.

B. Magnetoelastic coupling

Magnetostriction is caused by the coupling between the magnetic and elastic degrees of freedom. A theory for the magnetoelastic interaction in $RbMnF_3$ was presented by Eastman *et al.*[22,23] who studied the dependence of the antiferromagnetic resonance (AFMR) on uniaxial pressure. Their approach was used and extended by Melcher and Bolef[28] who investigated the effects of the magnetoelastic interaction on the sound velocities. The same theory will be used in the present section to interpret the observed magnetostriction in fields below ~ 4 kOe.

The volume dependence of the exchange interaction, which leads to exchange magnetostriction, was justifiably ignored by Eastman *et al.* Because the exchange magnetostriction is unimportant in fields below ~ 4 kOe, it will not be considered in the present section.[29]

According to Eastman,[22] the energy E_{ME} due to the magnetoelastic coupling in $RbMnF_3$ can be written[30]

$$E_{ME} = B_1[(\alpha_1^2+\beta_1^2)\epsilon_{11} + (\alpha_2^2+\beta_2^2)\epsilon_{22} + (\alpha_3^2+\beta_3^2)\epsilon_{33}] + B_2[(\alpha_1\alpha_2+\beta_1\beta_2)\epsilon_{12} + (\alpha_2\alpha_3+\beta_2\beta_3)\epsilon_{23} + (\alpha_3\alpha_1+\beta_3\beta_1)\epsilon_{31}]$$
$$+ B_3(\alpha_1\beta_1\epsilon_{11} + \alpha_2\beta_2\epsilon_{22} + \alpha_3\beta_3\epsilon_{33}) + B_4[(\alpha_1\beta_2+\alpha_2\beta_1)\epsilon_{12} + (\alpha_2\beta_3+\alpha_3\beta_2)\epsilon_{23} + (\alpha_3\beta_1+\alpha_1\beta_3)\epsilon_{31}], \quad (4)$$

where ϵ_{ij} are the strain coefficients. It is noteworthy that Eastman *et al.* use the engineering strain coefficients ϵ_{ij}, whereas some treatments of the magnetostriction in ferromagnets employ the strain tensor whose shear components are one-half the engineers' shear components.

Equation (4) is simplified considerably if one uses the low-H approximation in which $\vec{M}_1$ is antiparallel to $\vec{M}_2$. In this approximation, $\alpha_i = -\beta_i = \gamma_i$ so that

$$E_{ME} = 2b_1(\gamma_1^2\epsilon_{11} + \gamma_2^2\epsilon_{22} + \gamma_3^2\epsilon_{33}) + 2b_2(\gamma_1\gamma_2\epsilon_{12} + \gamma_2\gamma_3\epsilon_{23} + \gamma_3\gamma_1\epsilon_{31}), \quad (5)$$

where $b_1 = B_1 - \frac{1}{2}B_3$ and $b_2 = B_2 - B_4$.

C. Predicted magnetostriction

1. General expression

Equation (5) for magnetoelastic coupling at low H has the same form as the usual expression for the magnetoelastic coupling in cubic ferromagnets,[1,2] except that the direction cosines γ_i of the staggered magnetization $\vec{L}$ play the role of the direction cosines of the magnetization $\vec{M}$ in a ferromagnet. Owing to this formal similarity, one can apply the theoretical results for a cubic ferromagnet to the present case. This leads to the following expression for the fractional change in length $\delta l/l$ measured along the direction of the

unit vector $\hat{l}$:

$$\delta l/l = \tfrac{3}{2}\lambda_{100}(\gamma_1^2\eta_1^2 + \gamma_2^2\eta_2^2 + \gamma_3^2\eta_3^2 - \tfrac{1}{3}) + 3\lambda_{111}(\gamma_1\gamma_2\eta_1\eta_2 + \gamma_2\gamma_3\eta_2\eta_3 + \gamma_3\gamma_1\eta_3\eta_1), \quad (6)$$

where η_i are the direction cosines of $\hat{l}$,

$$\lambda_{100} = -4b_1/3(c_{11} - c_{12}), \quad (7)$$

$$\lambda_{111} = -2b_2/3c_{44}, \quad (8)$$

and c_{ij} are the usual elastic constants.

Several comments should be made in connection with Eq. (6): (i) This equation gives the fractional change in length $\delta l/l$ relative to the so-called "demagnetized state."[1] To calculate the fractional change in length caused by a given physical operation (such as a change in the magnitude or direction of $\vec{H}$) one should calculate the *change* in $\delta l/l$ caused by this operation. (ii) Equation (6) applies to a single domain in which γ_i, the direction cosines of $\vec{L}$, are uniquely determined. (iii) In contrast to the case of a ferromagnet at high fields (for which $\vec{M} \parallel \vec{H}$), γ_i are not the direction cosines of $\vec{H}$. In fact, when $H \gg H_{sf}$, $\vec{L}$ is perpendicular to $\vec{H}$. (iv) Apart from constant terms which do not depend on the direction of $\vec{L}$, Eq. (6) is identical with Eq. (20) of Melcher and Bolef.[28] (v) Equation (6) involves only two constants, λ_{100} and λ_{111}, and is adequate for the present purposes. A similar "two-constant approximation" is usually adequate for cubic ferromagnets. A more complete treatment[1,2] involves more than two constants. (vi) In the two-constant approximation, the volume of the sample does not depend on the orientation of the magnetization (or staggered magnetization in the case of an antiferromagnet). If one goes beyond this approximation, one obtains a volume change with a change in the γ_i, but an estimate shows that this volume change is very small in the present case (see Sec. V A).

Equation (6) will be used to calculate the magnetostriction associated with the H-induced reorientation of $\vec{L}$ at low H. Only the configurations of $\vec{H}$ and $\hat{l}$ which were studied experimentally in the present work will be considered. For all these configurations, $\hat{l}$ is parallel to the [001] axis so that only the change in the term $\frac{3}{2}\lambda_{100}\gamma_3^2\eta_3^2$ in Eq. (6) is relevant.

2. $\hat{l} \parallel \vec{H} \parallel [001]$

For this configuration, the fractional change of length $\Delta l/l$ induced by the magnetic field is the same for all four types of domains. At $H=0$, $\vec{L}$ is parallel to one of the $\langle 111 \rangle$ axes, so that $\gamma_3^2 = \frac{1}{3}$. For fields above H_{sf}, $\vec{L}$ is perpendicular to the [001] axis, so that $\gamma_3^2 = 0$. The fractional change in length $(\Delta l/l)_{sf}$ which occurs between $H=0$ and $H > H_{sf}$ is therefore given by

$$(\Delta l/l)_{sf} = -(1/2)\lambda_{100} = 2b_1/3(c_{11} - c_{12}). \quad (9)$$

Because the experimental value of b_1 in $RbMnF_3$ is positive,[22,28] as is $(c_{11} - c_{12})$, the predicted $(\Delta l/l)_{sf}$ is positive, i.e., the H-induced reorientation of $\vec{L}$ should lead to an elongation. Since this elongation is the same for all domains, the change in the length of the sample as a whole should also be given by Eq. (9).

3. $\hat{l} \parallel [001]$, $\vec{H} \parallel [100]$

For this configuration also, all the domains exhibit the same magnetostriction. At $H=0$, $\gamma_3^2 = \frac{1}{3}$. For fields above H_{sf}, $\vec{L}$ is parallel to the [011] direction or to the $[01\bar{1}]$ direction, so that $\gamma_3^2 = \frac{1}{2}$. The fractional change in length between $H=0$ and $H > H_{sf}$ is given by

$$(\Delta l/l)_{sf} = \tfrac{1}{4}\lambda_{100} = -b_1/3(c_{11} - c_{12}). \quad (10)$$

In this case $(\Delta l/l)_{sf}$ is negative, i.e., the H-induced reorientation of $\vec{L}$ leads to a contraction. The magnitude of this contraction is equal to half the elongation which occurs in the configuration $\hat{l} \parallel \vec{H} \parallel [001]$.

4. $\hat{l} \parallel [001]$, $\vec{H} \parallel [110]$

For this field direction, the four types of domains do not behave in a similar way. However, in all regions of the sample the staggered magnetization above 2.0 kOe is parallel to either the $[\bar{1}11]$ direction or to the $[1\bar{1}1]$ direction. For both of these directions, $\gamma_3^2 = \frac{1}{3}$, i.e., the same value as at $H=0$. This implies that the sample's length along the [001] direction for fields above 2.0 kOe is the same as at $H=0$.

The conclusion that the length above 2.0 kOe is the same as at $H=0$ does not necessarily imply that the length is constant between $H=0$ and 2 kOe. However, if the unstable domains disappear in fields of several hundred Oe, as suggested,[24] then no change in length is expected above several hundred Oe. Of course, at very high fields ($H \gg 10$ kOe), an appreciable exchange magnetostriction will occur.

5. *Effect of uniaxial compression*

In the preceding calculations of the magnetostriction it was assumed that the sample was not subjected to external mechanical stresses. However, as noted in Sec. II, the measurements in the present work were performed with the sample subjected to a uniaxial pressure of approximately 14 bar along the [001] direction. This pressure along the direction of $\hat{l}$ was exerted by three copper-beryllium springs which held the sample firmly in the capacitance cells used in the measurements. Although the uniaxial pressure was

relatively small, apparently it produced measurable changes in the magnetostriction. The effects of the uniaxial compression on the observed magnetostriction were calculated using the expressions given earlier for the anisotropy and magnetoelastic energies [Eqs. (3) and (5)].[31]

The effect of an external stress on the low-field magnetostriction can be explained qualitatively as follows. When a compressional stress is applied along the [001] direction, it produces a uniaxial anisotropy, in addition to the zero-stress cubic anisotropy which is given by Eq. (3). Experimentally,[22] the sign of the stress-induced anisotropy is such that a compression along [001] tends to align $\vec{L}$ parallel to the [001] direction (or to the [00$\bar{1}$] direction). Owing to this additional anisotropy, the equilibrium orientation of $\vec{L}$, both at $H=0$ and at finite H, depends on the uniaxial pressure p. This dependence is relatively strong in $RbMnF_3$ because the intrinsic cubic anisotropy is very weak so that the stress-induced anisotropy is very effective in changing the orientation of $\vec{L}$. Because the magnetostriction depends on the H-induced change in the orientation of $\vec{L}$, and because this change is p dependent, the results for $(\Delta l/l)_{sf}$ are p dependent.

The magnetostrictive strain under a constant external stress is still given by the same formal expression as at zero stress,[2] which is Eq. (6) in the "two-constant approximation" used in the present work. However, the γ_i which appear in Eq. (6) are now stress dependent. For the experimental configurations in the present study, only the p dependence of γ_3^2 need be considered. This dependence is calculated by adding a stress-induced anisotropy $E_A(p)$ to the intrinsic cubic anisotropy E_A which is given by Eq. (3), i.e., the effective anisotropy E_A^{eff} is given by

$$E_A^{\text{eff}} = E_A + E_A(p). \tag{11}$$

Using the expressions for the stress-induced anisotropy,[32] and specializing to the case of a uniaxial compression along the [001] direction, one obtains

$$E_A(p) = -2b_1 p\gamma_3^2/(c_{11}-c_{12}). \tag{12}$$

The equilibrium orientation of $\vec{L}$ at $H=0$ is calculated by minimizing the effective anisotropy energy [which is given by Eqs. (3), (11), and (12)] with respect to γ_i. At the minimum,

$$\gamma_3^2 = \tfrac{1}{3}[1 - 2b_1 p/K(c_{11}-c_{12})]. \tag{13}$$

In $RbMnF_3$, $K<0$ and $b_1>0$, so that γ_3^2 increases with increasing p, i.e., with increasing compression the staggered magnetization rotates from the [111] direction toward the [001] direction (or the equivalent for the other three types of domains). Ultimately, $\vec{L}$ becomes parallel to the [001] direction at a uniaxial pressure p_c which is given by

$$p_c = -K(c_{11}-c_{12})/b_1. \tag{14}$$

The data of Eastman[22] indicate that $p_c = 420$ bar. The reduced uniaxial pressure x is defined as

$$x = p/p_c = -pb_1/K(c_{11}-c_{12}). \tag{15}$$

In the present experiments p was approximately 14 bar, so that $x \cong 3.3\times 10^{-2}$. Equation (13) for the equilibrium orientation of $\vec{L}$ at $H=0$ may be rewritten

$$\gamma_3^2 = \tfrac{1}{3}(1+2x). \tag{16}$$

For fields well above H_{sf}, the equilibrium orientation of $\vec{L}$ is determined by minimizing the effective anisotropy energy in the plane perpendicular to $\vec{H}$.[17] We consider the three orientations of $\vec{H}$ used in the present work separately, and calculate the p dependence of $(\Delta l/l)_{sf}$ in each case.

When $\vec{H}$ is parallel to [001], the equilibrium orientation of $\vec{L}$ at $H>H_{sf}$ is not affected by the stress-induced anisotropy (although the value of H_{sf} does depend on p). Thus, $\gamma_3^2=0$ for $H>H_{sf}$. Combining Eqs. (6) and (16) one then obtains

$$(\Delta l/l)_{sf} = -\tfrac{1}{2}\lambda_{100}(1+2x). \tag{17}$$

Comparison with Eq. (9) indicates that the uniaxial pressure increases the magnitude of $(\Delta l/l)_{sf}$ by a factor $(1+2x)$, which is approximately equal to 1.067 for the present experiments. Note that $(\Delta l/l)_{sf}$ is positive for this experimental configuration, so that the uniaxial pressure makes a positive contribution to $(\Delta l/l)_{sf}$.

When $\vec{H}$ is parallel to [100], and $H>H_{sf}$, the minimization of E_A^{eff} in the (100) plane gives

$$\gamma_3^2 = \tfrac{1}{2}(1+x). \tag{18}$$

Combining Eqs. (6), (16), and (18), one obtains

$$(\Delta l/l)_{sf} = \tfrac{1}{4}\lambda_{100}(1-x). \tag{19}$$

Comparison of Eq. (19) with Eq. (10) indicates that the uniaxial pressure changes $(\Delta l/l)_{sf}$ by a factor $(1-x)$, which is approximately equal to 0.967 for the present experiments. Note that $(\Delta l/l)_{sf}$ is negative for this experimental configuration, so that also in this case the uniaxial pressure makes a positive contribution to $(\Delta l/l)_{sf}$.

When $\vec{H}$ is parallel to the [110] direction and H is above 2 kOe, γ_3^2 is given by the same expression as in the case $H=0$, namely, Eq. (16). Since the change in length along the [001] direction is proportional to the change in γ_3^2, it follows that above 2 kOe this length is the same as at $H=0$. The same result was derived earlier for the special case $p=0$.

D. Experimental results

The length l of the sample along the [001] direction was measured as a function of H. The field $\vec{H}$ was parallel to the [001], [100], or [110] directions. The low-field magnetostriction for the longitudinal configuration $\hat{l} \parallel \vec{H} \parallel [001]$ is shown in Fig. 3. In accordance with the theoretical prediction, the length l in fields above $H_{sf} \cong 2.5$ kOe is larger than at $H=0$. The magnitude of the fractional change in length is $(\Delta l/l)_{sf} = (1.57 \pm 0.13) \times 10^{-6}$. This value, and the one below, exclude the exchange magnetostriction which is discussed in Sec. V. The exchange-magnetostriction correction for $(\Delta l/l)_{sf}$ amounts to a mere 0.007×10^{-6} at 4 kOe. (Some of the low-field data, however, were taken in fields up to 9 kOe where the correction is 0.03×10^{-6}.)

Figure 4 shows the low-H magnetostriction for the two transverse configurations: (i) $\hat{l} \parallel [001]$ with $\vec{H} \parallel [100]$, and (ii) $\hat{l} \parallel [001]$ with $\vec{H} \parallel [110]$. For the first configuration, the length decreases as the field is changed from zero to a value above H_{sf}. For the second configuration there is no detectable change in length in fields up to 4 kOe. These results are in agreement with the theoretical predictions. The observed change in length when $\vec{H}$ is parallel to the [100] direction is $(\Delta l/l)_{sf} = -(0.67 \pm 0.05) \times 10^{-6}$. Thus, the experimental ratio between $(\Delta l/l)_{sf}$ with $\vec{H} \parallel [100]$ and that with $\vec{H} \parallel [001]$ is -0.43. The theoretically-predicted ratio (with the uniaxial pressure of 14 bar along [001] taken into account) is -0.45.

The magnetostriction data, such as those shown in Figs. 3 and 4, showed no hysteresis, i.e., they were the same for increasing and decreasing H. Also, there was no change in the results when the direction of $\vec{H}$ was reversed. From the theoretical discussion it follows that for all the experimental configurations which were studied, $(\Delta l/l)_{sf}$ should not have depended on the relative populations of the four types of $\langle 111 \rangle$ domains at $H=0$. Thus, the absence of hysteresis does not necessarily imply that a magnetic field cycle had no effect on the distribution of domains. For example, it is not possible to say whether the [111] and [11$\bar{1}$] domains, which were unstable at high fields when $\vec{H}$ was

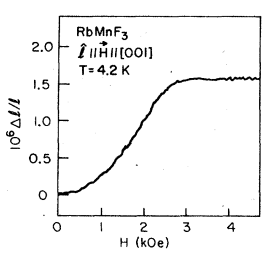

FIG. 3. Recorder trace of the low-field magnetostriction of $RbMnF_3$ at 4.2 K. These data are for the longitudinal configuration, $\hat{l} \parallel \vec{H} \parallel [001]$.

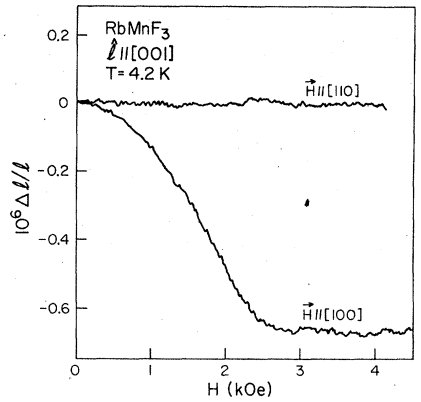

FIG. 4. Low-field transverse magnetostriction of $RbMnF_3$ at 4.2 K. The two traces correspond to the configurations: (i) $\hat{l} \parallel [001]$ with $\vec{H} \parallel [100]$, and (ii) $\hat{l} \parallel [001]$ with $\vec{H} \parallel [110]$.

parallel to the [110] direction, reappeared when H was subsequently reduced to zero.

E. Magnetoelastic coupling constant

Previous investigations[22,28] have established that the magnetoelastic coupling constant b_1 in $RbMnF_3$ is an order of magnitude larger than b_2. In the present work, the values of $(\Delta l/l)_{sf}$ were used to determine b_1 at 4.2 K. Here, use was made of Eqs. (7), (17), and (19), the value $x = 3.33 \times 10^{-2}$ for the present experiments, and the measured elastic constants.[33] The value of $(\Delta l/l)_{sf}$ for the longitudinal configuration, $\hat{l} \parallel \vec{H} \parallel [001]$, gave $b_1 = (1.88 \pm 0.15) \times 10^6$ erg/cm^3. The value of $(\Delta l/l)_{sf}$ for the transverse configuration, $\hat{l} \parallel [001]$ with $\vec{H} \parallel [100]$, gave $b_1 = (1.77 \pm 0.14) \times 10^6$ erg/cm^3.

Eastman's original determination of b_1 from AFMR measurements under stress[22] gave $b_1 = (1.5 \pm 0.15) \times 10^6$ erg/cm^3. However, as pointed out by Melcher and Bolef,[28] the elastic constants used by Eastman were inaccurate. Correcting for this, Eastman's value is $b_1 = (1.8 \pm 0.18) \times 10^6$ erg/cm^3. From the H dependence of the sound velocities, Melcher and Bolef[28] obtained $b_1 = (1.95 \pm 0.15) \times 10^6$ erg/cm^3. All these values are for $T = 4.2$ K. It is apparent that the values of b_1 obtained from the magnetostriction measurements in the present work are in good agreement with previous determinations of the same parameter.

V. MAGNETOSTRICTION AT HIGH FIELDS

Section IV was devoted to the magnetostriction associated with the reorientation of $\vec{L}$, which is completed in fields of several kOe. In the present section the magnetostriction at higher fields is discussed. It can be shown that apart from the change $(\Delta l/l)_{sf}$ which occurs at low fields, the

magnetostriction at high fields, and for a given magnitude of H, is very nearly independent of the directions of $\vec{H}$ and $\hat{l}$. However, in what follows we shall consider explicitly only the magnetostriction above H_{sf} when $\vec{H}$ is parallel to one of the $\langle 100 \rangle$ directions and when $\hat{l}$ is parallel to [001].

A. Theory

It will be shown that the magnetostriction in fields above H_{sf} arises from the strain dependence of the exchange interaction. In $RbMnF_3$, the only significant exchange interaction is between nearest-neighbor spins. Thus, the Hamiltonian for the exchange interaction may be written

$$\mathcal{H}_E = -\sum 2J\vec{S}_i \cdot \vec{S}_j , \tag{20}$$

where J is the exchange "constant" between nearest neighbors i and j, and the sum is over all pairs of nearest neighbors. The strain dependence of the exchange interaction arises from the dependence of J on interatomic distances.

Two alternative methods of calculating the magnetostriction above H_{sf} are presented below. Each of these methods has advantages.

1. Relations between the magnetostriction and the magnetic Grüneisen constant

Consider a $RbMnF_3$ sample at zero external mechanical stress. Let the volume at $H=0$ be $V(0)$. The H dependence of the volume V can be calculated from a Maxwell relation which is obtained from the thermodynamic potential $\Phi(T, P, H)$, namely,

$$\left(\frac{\partial V}{\partial H}\right)_{T,P} = -\left(\frac{\partial I}{\partial P}\right)_{T,H} , \tag{21}$$

where I is the component of the total magnetic moment of the sample along the direction of $\vec{H}$, and P is the hydrostatic pressure. (Note that the total magnetic moment is the product of the magnetization and V.) Let $I = \chi V(0) H$, then Eq. (21) may be written

$$\frac{1}{V(0)}\left(\frac{\partial V}{\partial H}\right)_{T,P} = -H\left(\frac{\partial \chi}{\partial P}\right)_{T,H} . \tag{22}$$

It should be noted that whereas the symbol χ is often reserved for the susceptibility per unit volume, its meaning here is somewhat different, because in the definition $\chi = I/V(0)H$ the denominator contains $V(0) \equiv V(H=0, P=0)$ rather than V. Thus, χ is the susceptibility per unit $V(0)$, rather than per unit V.

For fields $H_{sf} < H \ll 2H_E \cong 1600$ kOe, the susceptibility $\chi(T, P, H)$ is very nearly independent of H. Therefore, above H_{sf} but below our maximum field of 137 kOe, $\partial\chi/\partial P$ is independent of H and (for a given T and P) can be taken as a constant.

The susceptibility above H_{sf} is designated as $\chi_\perp$, because at these fields $\vec{L}$ is perpendicular to $\vec{H}$. Integrating Eq. (22) between H_{sf} and H, one obtains

$$[V(H) - V(H_{sf})]/V(0) = -\tfrac{1}{2}(\partial\chi_\perp/\partial P)(H^2 - H_{sf}^2) , \tag{23}$$

where it is understood that the temperature is fixed.

The volume magnetostriction ($\Delta V/V$) is defined as

$$\Delta V/V = [V(H) - V(0)]/V(0) . \tag{24}$$

Equation (23) therefore indicates that above H_{sf}, $\Delta V/V$ varies linearly with H^2, and

$$\frac{d(\Delta V/V)}{d(H^2)} = -\frac{1}{2}\left(\frac{\partial \chi_\perp}{\partial P}\right) . \tag{25}$$

In mean-field theory, the perpendicular susceptibility for all $T < T_N$ is given by

$$\chi_\perp^{MF} = -ng^2\mu_B^2/4zJV(0) , \tag{26}$$

where n is the number of magnetic ions in the sample, g is the g factor, μ_B is the Bohr magneton, and z is the number of nearest neighbors. In Eq. (26), a term of order $H_A/H_E \sim 10^{-5}$ was neglected in comparison with unity.[34] Going beyond the mean-field approximation, the perpendicular susceptibility at $T=0$ is given by

$$\chi_\perp(T=0) = \chi_\perp^{MF}(1-f) , \tag{27}$$

where f is a correction due to zero-point spin deviations (see Refs. 35 and 36). For $RbMnF_3$, $f=0.05$. It is significant that f does not depend on the hydrostatic pressure P. Because the present experiments were performed at $T \ll T_N$, $\chi_\perp$ was practically identical with $\chi_\perp(T=0)$, so that Eq. (27) may be applied.

Assuming that the pressure dependence of the g factor is negligible in comparison with the pressure dependence of J (which is expected to be true for $RbMnF_3$), the P dependence of $\chi_\perp$ arises solely from the P dependence of J. Because $\chi_\perp \propto 1/J$, it follows that

$$\frac{1}{\chi_\perp}\left(\frac{\partial \chi_\perp}{\partial P}\right) = -\frac{1}{J}\left(\frac{\partial J}{\partial P}\right) = \left(\frac{\partial \ln J}{\partial \ln V}\right)\kappa , \tag{28}$$

where κ is the compressibility. The magnetic Grüneisen constant γ_{mag} (not to be confused with the direction cosines γ_i) is defined as

$$\gamma_{mag} = -(\partial \ln J/\partial \ln V) . \tag{29}$$

From Eqs. (25), (28), and (29) it follows that for $H > H_{sf}$,

$$\frac{d(\Delta V/V)}{d(H^2)} = \tfrac{1}{2}\chi_\perp \kappa \gamma_{\mathrm{mag}}. \tag{30}$$

We now show that the volume change above H_{sf} is associated with equal fractional changes in all linear dimensions of the sample. The H-induced change in any linear dimension of the sample at fields above H_{sf} can be calculated along similar lines as those used to calculate the change in V. The essential difference is that the derivative of χ with respect to the hydrostatic pressure P is replaced by the derivative with respect to the uniaxial pressure p applied along $\hat{l}$. Thus, the analog of Eq. (23) is

$$\frac{l(H) - l(H_{sf})}{l(0)} = -\frac{1}{2}\left(\frac{\partial \chi_\perp}{\partial p}\right)(H^2 - H_{sf}^2). \tag{31}$$

In $RbMnF_3$, each Mn^{++} ion is surrounded by six nearest neighbors on the opposite sublattice. Two of these neighbors are situated along the [001] direction, while the other four are situated along the [100] and [010] directions. When a uniaxial pressure p is applied along the [001] direction, the distances to the first two neighbors are shortened, whereas the distances to the other four neighbors become longer. Thus, the exchange "constant" J which characterizes the interaction with each of the two ions along [001] is changed by an amount $j_1(p)$, while the exchange "constant" for the interaction with the other four neighbors is changed by $j_2(p)$. In principle, a uniaxial pressure along [001] changes the symmetry of the crystal from cubic to tetragonal, so that j_1 and j_2 may be second-rank tensors rather than scalars. However, for $RbMnF_3$ we expect that the exchange interaction is very nearly isotropic even when a uniaxial pressure is applied.[37] We, therefore, assume that j_1 and j_2 are scalars, i.e., the exchange interactions are isotropic even for $p \neq 0$. Because the susceptibility $\chi_\perp$ above H_{sf} depends almost entirely on the exchange interactions (and only very weakly on the anisotropy, whether intrinsic or stress induced), it follows that $\chi_\perp(p)$ is isotropic, i.e., it does not depend on the direction of $\vec{H}$. Thus, the derivative $\partial\chi_\perp/\partial p$ remains unchanged when the direction of $\vec{H}$ is changed from [001] to [100] while the direction of the uniaxial pressure is kept fixed along the [001] direction. It then follows from Eq. (31) that for a given magnitude of H, the change in the length l along the [001] direction, measured relative to $l(H_{sf})$, is the same for both $\vec{H} \parallel [001]$ and $\vec{H} \parallel [100]$. An equivalent statement is that if $\vec{H}$ is parallel to [001], then the fractional change in length above H_{sf} is the same for both $\hat{l} \parallel [001]$ and $\hat{l} \parallel [100]$.

Because the fractional changes in length above H_{sf} are the same for all three $\langle 100 \rangle$ directions, it follows that each fractional change in length is equal to one third of the fractional change in volume. Thus, for both the longitudinal configuration, $\hat{l} \parallel \vec{H} \parallel [001]$, and the transverse configuration, $\hat{l} \parallel [001]$ with $\vec{H} \parallel [100]$, one obtains from Eqs. (23), (25), and (30),

$$\frac{l(H) - l(H_{sf})}{l(0)} = -\frac{1}{6}\left(\frac{\partial \chi_\perp}{\partial P}\right)(H^2 - H_{sf}^2) \tag{32}$$

and

$$\frac{d(\Delta l/l)}{d(H^2)} = -\frac{1}{6}\left(\frac{\partial \chi_\perp}{\partial P}\right) = \frac{1}{6}\chi_\perp \kappa \gamma_{\mathrm{mag}}. \tag{33}$$

The interpretation of the high-field magnetostriction data will be based primarily on Eqs. (32) and (33) which are valid only for $H > H_{sf}$. For completeness, we have also calculated the magnetostriction between $H = 0$ and $H = H_{sf}$ by means of Eq. (21) and its analog for the derivative $\partial l/\partial H$. A zero external mechanical stress was assumed. We quote the results, but omit the derivations.

With $\vec{H}$ parallel to [001], the volume change between $H = 0$ and $H = H_{sf}$ is given by

$$\frac{V(H_{sf}) - V(0)}{V(0)} = -\frac{1}{2}\left(\frac{\partial \chi_\perp}{\partial P}\right) H_{sf}^2 - \frac{1}{6}\left(\frac{\partial K}{\partial P}\right). \tag{34}$$

Both terms on the right-hand side of Eq. (34) are quite small. Using the experimental results below, the first term is equal to 8×10^{-9}. The second term was estimated by assuming that $-(\partial \ln K/\partial \ln V)$ is of order 5, which gave a contribution of $\sim 1 \times 10^{-9}$ to the fractional change in volume. As noted earlier, Eq. (6) in Sec. IV gives a zero volume change between $H = 0$ and $H = H_{sf}$. The discrepancy between Eq. (6) and (34) is due to two reasons. First, in the derivation of Eq. (6), the exchange magnetostriction [which gives rise to the first term on the right-hand side of Eq. (34)] was neglected. Second, Eq. (6) represents the "two-constant approximation" to the low-field magnetostriction (which is quite adequate for the present purposes). A more complete treatment (see Refs. 1 or 2) leads to a formula with five constants which, in turn, leads to the term $-\frac{1}{6}(\partial K/\partial P)$. By combining Eqs. (23), (25), (30), and (34), one obtains

$$\frac{\Delta V}{V} = \frac{V(H) - V(0)}{V(0)} = \tfrac{1}{2}\chi_\perp \kappa \gamma_{\mathrm{mag}} H^2, \tag{35}$$

where the small term involving $\partial K/\partial P$ was omitted. Equation (35) is valid only for $H > H_{sf}$.

The change in length between $H = 0$ and $H = H_{sf}$

was calculated for the longitudinal configuration, $\hat{l} \parallel \vec{H} \parallel [001]$, and for the transverse configuration, $\hat{l} \parallel [001]$ with $\vec{H} \parallel [100]$. Omitting a small term involving $\partial K/\partial P$, one obtains for either configuration

$$\frac{l(H_{sf}) - l(0)}{l(0)} = \left(\frac{\Delta l}{l}\right)_{sf} - \frac{1}{6}\left(\frac{\partial \chi_\perp}{\partial P}\right) H_{sf}^2 , \tag{36}$$

where $(\Delta l/l)_{sf}$ depends on the configuration and is given by Eqs. (9) and (10) of Sec. IV. The second term in Eq. (36) represents a (small) correction due to the exchange magnetostriction. Combining Eqs. (32), (33), and (36), one obtains for $H > H_{sf}$,

$$\frac{\Delta l}{l} = \frac{l(H) - l(0)}{l(0)} = \left(\frac{\Delta l}{l}\right)_{sf} + \tfrac{1}{6}\chi_\perp \kappa \gamma_{mag} H^2 . \tag{37}$$

2. Relation between the magnetostriction and the two-spin correlation function

An alternative approach to the calculation of the magnetostriction above H_{sf} is based on the work of Callen and Callen.[4,5] In this approach the magnetostriction is expressed in terms of certain spin correlation functions, and coupling terms which are strain-derivatives of the anisotropy and exchange "constants." This method leads to particularly simple results when the following conditions are met: (i) the exchange interactions are between nearest neighbors only, and are described by the Hamiltonian in Eq. (20) with a strain-dependent scalar J, (ii) the anisotropy is zero, and (iii) the material is cubic. Under these assumptions the fractional change in volume, $\delta V/V$, due to the magnetic interaction is related to the accompanying change $\delta\langle \vec{S}_i \cdot \vec{S}_j \rangle$ in the static two-spin correlation function $\langle \vec{S}_i \cdot \vec{S}_j \rangle$ between nearest neighbors. The relation is [see Eq. (5) of Ref. 3]

$$\delta V/V = -n z \kappa J \gamma_{mag} \delta\langle \vec{S}_i \cdot \vec{S}_j \rangle / V(0) . \tag{38}$$

Equation (38) is not restricted to isothermal changes in V. Thus, a change in $\langle \vec{S}_i \cdot \vec{S}_j \rangle$ which is caused by a variation of either T and/or H leads to a change in V which is given by Eq. (38). In the special case of a fixed T, Eq. (38) relates the magnetostriction to the H-induced change in $\langle \vec{S}_i \cdot \vec{S}_j \rangle$. It has been shown[3] that in this special case, the magnetostriction as given by Eq. (38) is the same as the one calculated from Eq. (21).

Another special case is a variation of T at $H = 0$. The magnetic part of the change in volume between the temperatures T_1 and T_2 is then proportional to the change in the exchange energy between these two temperatures. Thus, the magnetic part of the thermal expansion coefficient at $H = 0$ is proportional to the magnetic part of the specific heat. This prediction was verified in experiments on the ferromagnet EuO.[6]

Consider the change in the sample's length l which occurs as the sample is cooled from a temperature $T \gg T_N$ to $T = 0$, while keeping $H = 0$. The integrated fractional change in length $(\delta l/l)_0$ associated with this cooling process is related to the change in $\langle \vec{S}_i \cdot \vec{S}_j \rangle$. The correlation function $\langle \vec{S}_i \cdot \vec{S}_j \rangle$ is proportional to the exchange energy. Therefore, for an antiferromagnet at $T = H = 0$, this correlation function is given by

$$\langle \vec{S}_i \cdot \vec{S}_j \rangle = -S^2(1 + e_0/zS) , \tag{39}$$

where e_0/zS is a correction term for the ground-state energy of an antiferromagnet and is equal to 0.04 in $RbMnF_3$.[36] For $T \gg T_N$, $\langle \vec{S}_i \cdot \vec{S}_j \rangle$ is negligible. Therefore, from Eqs. (38) and (39), $(\delta l/l)_0$ is given by

$$\left(\frac{\delta l}{l}\right)_0 = \frac{1}{3}\left(\frac{\delta V}{V}\right)_0 = \frac{\frac{1}{3} n z \kappa J \gamma_{mag} S^2 (1 + e_0/zS)}{V(0)} . \tag{40}$$

Equation (40) is expected to hold in the case of $RbMnF_3$ because the assumptions leading to this equation are well satisfied in this material. Also, the magnetostriction above H_{sf} in $RbMnF_3$ is expected to obey Eq. (38).

B. Experimental results

High-field magnetostriction measurements, up to 137 kOe, were performed at 4.2 K. The magnetostriction was measured for two configurations: (i) the parallel (longitudinal) configuration, with $\hat{l} \parallel \vec{H} \parallel [001]$, and (ii) a transverse configuration, with $\hat{l} \parallel [001]$ and $\vec{H} \parallel [100]$. For either configuration, the magnetostriction $\Delta l/l$ above $H_{sf} \simeq 2.5$ kOe varied linearly with H^2. The results for both configurations are shown in Fig. 5. The slope $d(\Delta l/l)/d(H^2)$ for the parallel configuration was

$$\left(\frac{d(\Delta l/l)}{d(H^2)}\right)_\parallel = (4.20 \pm 0.34) \times 10^{-16}\ \text{Oe}^{-2} .$$

For the transverse configuration, the slope was

$$\left(\frac{d(\Delta l/l)}{d(H^2)}\right)_\perp = (3.94 \pm 0.32) \times 10^{-16}\ \text{Oe}^{-2} .$$

C. Magnetic Grüneisen constant

The theory in Sec. V A shows that the slope $d(\Delta l/l)/d(H^2)$ for the parallel configuration should be equal to that for the perpendicular configuration, and should be related to the magnetic Grüneisen constant γ_{mag} by Eq. (33). Experimentally, the two slopes agree with each other within the experimental error. To obtain γ_{mag}, we use the average of the two slopes, namely, 4.07×10^{-16} Oe^{-2}. Substituting the measured susceptibility[35]

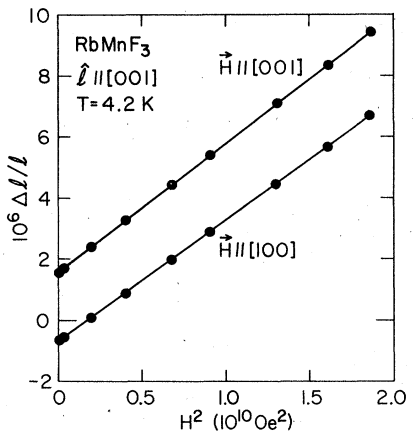

FIG. 5. High-field magnetostriction of $RbMnF_3$ at 4.2 K, plotted vs H^2. These data are for fields $H_{sf} < H < 137$ kOe. where $H_{sf} \cong 2.5$ kOe. The upper set of data are for the longitudinal configuration, $\hat{l} \parallel \vec{H} \parallel [001]$. The lower set of data are for a transverse configuration, $\hat{l} \parallel [001]$ with $\vec{H} \parallel [100]$.

and the compressibility,[33] Eq. (33) then gives

$$\gamma_{mag} = 4.5 \pm 0.4 .$$

The pressure dependence of the Neél temperature calculated from this value is $dT_N/dP = 0.53 \pm 0.05$ K/kbar. Our value for γ_{mag} will now be compared to other data which are related to this parameter.

The first attempt to determine γ_{mag} in $RbMnF_3$ was made by Golding[38] who measured the linear thermal expansion coefficient near T_N. From Eq. (38), the ratio α_{mag}/C_{mag} between the magnetic part of the thermal expansion coefficient and the magnetic specific heat per unit volume should be a constant equal to $\frac{1}{3}\kappa\gamma_{mag}$. Experimentally, Golding found that the ratio between his γ_{mag} and the C_{mag} obtained by Teaney *et al.*[39] was temperature dependent. Nevertheless, the asymptotic ratio for temperatures near T_N was used to obtain $\gamma_{mag} = 3.14 \pm 0.3$. This value is in disagreement with the present determination of γ_{mag}.

de Jongh and Breed[35] measured $\chi_\perp$ between 6 and 295 K. Analysis of the data for $T > T_N$ in terms of high-temperature series expansions for χ indicated that the exchange "constant" J was temperature dependent. This temperature dependence was attributed to the temperature dependence of the lattice constant $a(T)$, which had been previously measured by Teaney *et al.*[39] A comparison between $J(T)$ and $a(T)$ gave $dJ/da = 12 \pm 4$ K/Å. Using the measured exchange constant[16,35] $J = -3.4$ K and the lattice parameter $a = 4.23$ Å, this gives $\gamma_{mag} = 5.0 \pm 1.7$. This value is consistent with the present determination of γ_{mag}.

de Jongh and Block[40] analyzed the variation of the exchange "constant" J between nearest neighbors with bond length R. A series of insulating antiferromagnetic compounds $X MnF_3$ and $X MnF_4$, in which the superexchange paths connecting nearest magnetic neighbors were identical collinear (180°) Mn-F-Mn bonds, was considered in this analysis. Assuming that $|J|$ varied as R^{-m}, they obtained $m \cong 12$, which corresponds to $\gamma_{mag} \cong 4$. Another study of J as a function of the lattice parameter[41] gave $dJ/da \cong 11$ K/Å, corresponding to $\gamma_{mag} \cong 4.6$. These results are consistent with the value of γ_{mag} obtained in the present study.

Equation (40) relates γ_{mag} to the change in the lattice parameter (due to the magnetic interaction only) which occurs as the sample is cooled from $T \gg T_N$ to $T = 0$ in the absence of a magnetic field. Our result, $\gamma_{mag} = 4.5 \pm 0.4$, leads to $(\delta l/l)_0 = -(5.1 \pm 0.5) \times 10^{-4}$, where the minus sign indicates a contraction due to the antiferromagnetic order. However, the x-ray data of Teaney *et al.*[39] show no apparent magnetic lattice contraction, within an experimental resolution of $\sim 3 \times 10^{-4}$. To resolve this discrepancy, we have measured the thermal expansion of $RbMnF_3$ from 4.2 K to room temperature. A capacitance dilatometer made of copper was used, so that the measured quantity was the thermal expansion of $RbMnF_3$ relative to that of copper. The results indicated that $(\delta l/l)_0 = -(4.7 \pm 0.8) \times 10^{-4}$, which is consistent with the value obtained from our γ_{mag}, but is inconsistent with the data of Teaney *et al.* We note that the magnitude of $(\delta l/l)_0$ in $RbMnF_3$, observed here, is of the same order of magnitude as that in the antiferromagnets MnO and MnS (Ref. 15) and in the ferromagnets EuO and EuS (Refs. 3, 6, and 42). Our determination of γ_{mag} from the high-field magnetostriction data is believed to be more accurate than that from our thermal-expansion data.

ACKNOWLEDGMENTS

We wish to thank A. Platzker for providing the sample, S. Foner for valuable comments, and V. Diorio for technical assistance. This work was supported by the NSF.

*On leave from the University of São Paulo, São Paulo, Brazil.

[1] E. W. Lee, Rep. Prog. Phys. 18, 184 (1955).
[2] W. J. Carr, Jr., in *Handbuch der Physik*, edited by S. Flügge (Springer-Verlag, Berlin, 1966), Vol. XVIII/2.
[3] Y. Shapira, R. D. Yacovitch, C. C. Becerra, S. Foner, E. J. McNiff, Jr., D. R. Nelson, and L. Gunther, Phys. Rev. B 14, 3007 (1976).

[4]E. Callen and H. B. Callen, Phys. Rev. 139, A455 (1965).
[5]E. Callen, J. Appl. Phys. 39, 519 (1968).
[6]B. E. Argyle, N. Miyata, and T. D. Schultz, Phys. Rev. 160, 413 (1967).
[7]L. Alberts and E. W. Lee, Proc. Phys. Soc. Lond. 78, 728 (1961).
[8]R. Z. Levitin, A. S. Pakhomov, and V. A. Shchurov, Zh. Eksp. Teor. Fiz. 56, 1242 (1969) [Sov. Phys.–JETP 29, 669 (1969)]; see also, R. A. Voskanyan, R. Z. Levitin, and V. A. Shchurov, *ibid.* 54, 790 (1968) [*ibid.* 27, 423 (1968)].
[9]K. L. Dudko, V. V. Eremenko, and L. M. Semenenko, Phys. Status Solidi B 43, 471 (1971).
[10]R. D. Yacovitch and Y. Shapira, Physica (Utr.) 86-88B, 1126 (1977).
[11]G. J. Butterworth, J. A. Woollam, and P. Aron, Physica (Utr.) 70, 547 (1973).
[12]Y. Shapira, R. D. Yacovitch, and D. R. Nelson, Solid State Commun. 17, 175 (1975).
[13]Y. Shapira and R. D. Yacovitch, AIP Conf. Proc. 29, 435 (1976).
[14]Y. Shapira, R. D. Yacovitch, C. C. Becerra, S. Foner, and E. J. McNiff, Jr., Phys. Lett. A 55, 363 (1976).
[15]See, for example, B. Morosin, Phys. Rev. B 1, 236 (1970).
[16]C. G. Windsor and R. W. H. Stevenson, Proc. Phys. Soc. Lond. 87, 501 (1966).
[17]D. T. Teaney, M. J. Freiser, and R. W. H. Stevenson, Phys. Rev. Lett. 9, 212 (1962).
[18]There are discrepancies of up to ~15% between values of the exchange field obtained in different experiments, such as in Refs. 16 and 17. The value $H_E \cong 800$ kOe is sufficiently accurate for present purposes.
[19]L. J. de Jongh and A. R. Miedema, Adv. Phys. 23, 1 (1974).
[20]R. R. Birss and E. W. Lee, Proc. Phys. Soc. Lond. 76, 502 (1960).
[21]See, for example, N. F. Oliveira, Jr., S. Foner, Y. Shapira, and T. B. Reed, Phys. Rev. B 5, 2634 (1972).
[22]D. E. Eastman, Phys. Rev. 156, 645 (1967); see also, D. E. Eastman, R. J. Joenk, and D. T. Teaney, Phys. Rev. Lett. 17, 300 (1966).
[23]D. E. Eastman and M. W. Shafer, J. Appl. Phys. 38, 1274 (1967).
[24]P. H. Cole and W. J. Ince, Phys. Rev. 150, 377 (1966).
[25]A. Platzker, Ph.D. thesis (Electrical Engineering Dept., MIT, 1970) (unpublished).
[26]E. G. Petrov and V. N. Kharkyanen, Phys. Status Solidi B 50, K27 (1972).
[27]See, for example, Y. Shapira and S. Foner, Phys. Rev. B 1, 3083 (1970).
[28]R. L. Melcher and D. I. Bolef, Phys. Rev. 186, 491 (1969).
[29]A minor correction due to the exchange magnetostriction at low H is discussed later. Another contribution to the magnetostriction which is neglected here is the so-called "form effect" which depends on the shape of the sample. It can be shown that in the present experiments the form effect was negligible.
[30]Equations (4) and (5) express the magnetoelastic energy E_{ME} in terms of the strains. In the terminology of Ref. 2, E_{ME} represents the magnetoelastic energy term in the free energy F which is the analog of the Helmholtz function for ordinary materials. However, this terminology is not universal.
[31]We neglect terms in the magnetoelastic coupling which are quadratic in ϵ_{ij}. These "morphic energy terms" were discussed by W. P. Mason [Phys. Rev. 82, 715 (1951)] and in Ref. 2. Usually the effects due to the morphic energy terms are small. In two previous studies of the magnetoelastic interaction in $RbMnF_3$ (Refs. 22 and 28) the experimental findings were interpreted successfully by including only the magnetoelastic terms which appear in Eq. (5), i.e., terms linear in ϵ_{ij}. It can be shown that the relative contribution of the morphic energy terms to the stress dependence of the magnetostriction is comparable to the relative contributions of these energy terms to the effects studied in Refs. 22 and 28. The experimental findings in Refs. 22 and 28 therefore indicate that the morphic energy terms need not be included in the present work.
[32]See Eq. (15.20) of Ref. 2. In this reference $E_A(p)$ is called the "stress energy," and is designated as G_1 to indicate that it is that part of the Gibbs-like free energy which varies linearly with external mechanical stress. In Ref. 1, $E_A(p)$ is included in Eq. (6.1) and is called the "magnetoelastic energy."
[33]R. L. Melcher and D. I. Bolef, Phys. Rev. 178, 864 (1969).
[34]This also implies that terms involving $\partial H_A/\partial P$ will be neglected in comparison with terms involving $\partial H_E/\partial P$. Using the low-field data for the change in volume between $H=0$ and $H=H_{sf}$, and Eq. (34), it can be shown that the error introduced by this approximation is less than 0.1%.
[35]L. J. de Jongh and D. J. Breed, Solid State Commun. 15, 1061 (1974).
[36]F. Keffer, in *Handbuch der Physik*, edited by S. Flügge (Springer-Verlag, Berlin, 1966), Vol. XVIII/2.
[37]The exchange interaction between Mn^{++} ions in noncubic antiferromagnets, such as MnF_2, is well described by a scalar exchange constant. Moreover, in $RbMnF_3$ any significant stress-induced exchange anisotropy would have affected the results at low H, and would have led to substantially larger values of b_1 than that observed.
[38]B. Golding, J. Appl. Phys. 42, 1381 (1971).
[39]D. T. Teaney, V. L. Moruzzi, and B. E. Argyle, J. Appl. Phys. 37, 1122 (1966).
[40]L. J. de Jongh and R. Block, Physica (Utr.) 79B, 568 (1975).
[41]D. J. Breed, K. Gilijamse, J. W. E. Sterkenburg, and A. R. Miedema, Physica (Utr.) 68, 303 (1973).
[42]F. Lévy, Phys. Konden. Mater. 10, 71 (1969).